The East Greenland Boundary Current System South of Denmark Strait

J. Alexander Brearley[1], Robert S. Pickart[2], Hedinn Valdimarsson[3,4], Steingrimur Jonsson[4], Raymond W. Schmitt[2], T.W. Haine[5]

[1]National Oceanography Centre Southampton, Waterfront Campus, University of Southampton, European Way, Southampton, SO14 3ZH, United Kingdom, jab5@noc.soton.ac.uk
[2]Woods Hole Oceanographic Institution, Woods Hole, Massachusetts, United States
[3]Marine Research Institute, Reykjavik, Iceland
[4]University of Akureyri, Akureyri, Iceland
[5]Morton K. Blaustein Department of Earth and Planetary Sciences, Johns Hopkins University, Olin Hall, 34th and North Charles St., Baltimore, Maryland, United States
http://www.personal.soton.ac.uk/~jab5

1 Introduction

Along the East Greenland Shelf Break to the south of Denmark Strait there exists a sharp hydrographic front separating cold and fresh Arctic-origin water from warm and salty Atlantic-origin water (Figure 1). This front and its associated jet - known as the East Greenland Irminger Current - is one of the main routes by which fresh water and intermediate density Arctic water is advected southwards into the North Atlantic. It has been long established that the front and its jet are both highly variable in time and unstable, with lenses of Irminger Water being observed on the inshore side of the front in the early 20th century (Defant, 1930). Such cross-frontal exchange with the open Atlantic may be driven either by strong down-front barrier winds adjacent to the Greenland Plateau, or by instability of the boundary current.

In the period 2001-2007, four high resolution hydrographic/velocity sections were made during summer across the shelf and continental slope close to 66°N (Figure 2). These were designed to resolve the detailed cross-stream structure of the boundary current for the first time and to determine the shelf-basin exchange processes taking place. These efforts have been extended further by year-long monitoring of the boundary current (Harden and Pickart, 2011).

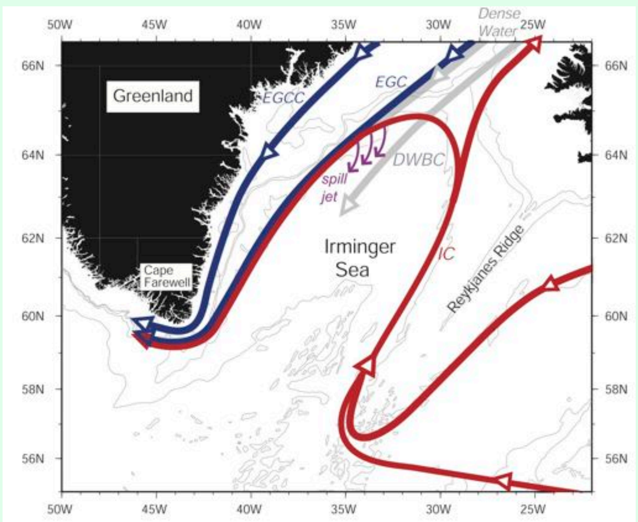

Figure 1: Boundary currents of the Irminger Sea. IC = Irminger Current; EGC = East Greenland Current; DWBC = Deep Western Boundary Current, along with the spill jet.

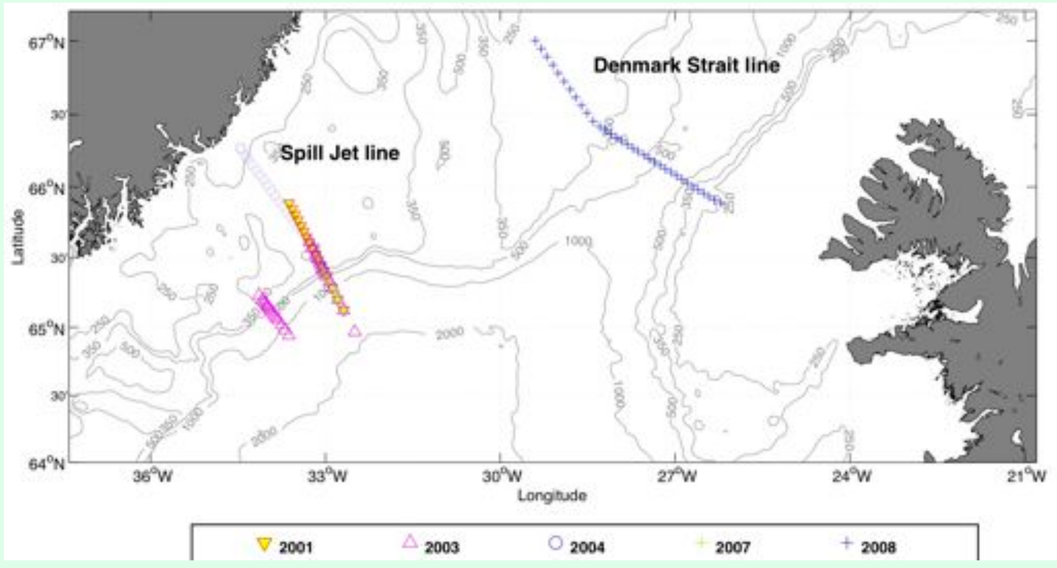

Figure 2: Positions of the hydrographic stations occupied during the four crossings of the boundary current.

2 Structure of the Boundary Current

From the four occupations, mean sections of potential temperature, salinity and absolute geostrophic velocity were constructed (Figure 3). The EGIC can be identified as a strong surface intensified current flowing equatorward close to the shelf break, whilst the DWBC is seen near the base of the continental slope. A third component of the boundary current system, first identified in a single section by Pickart et al. (2005), is a bottom-intensified velocity maximum in the vicinity of the shelf break and upper slope. This "spill jet" (Figure 3a) is thought to formed by dense water on the outer shelf cascading over the shelf break onto the upper slope, providing a route by which Arctic-origin water can enter the interior of the basin. The cross-shelf exchange process appears to be two way, with warm and salty lenses of Irminger Water observed shoreward of the main front in all four years. The spill jet itself also appears to be a persistent feature, being observed in all four occupations with a volume transport as large or larger than the DWBC at this latitude (Table 1).

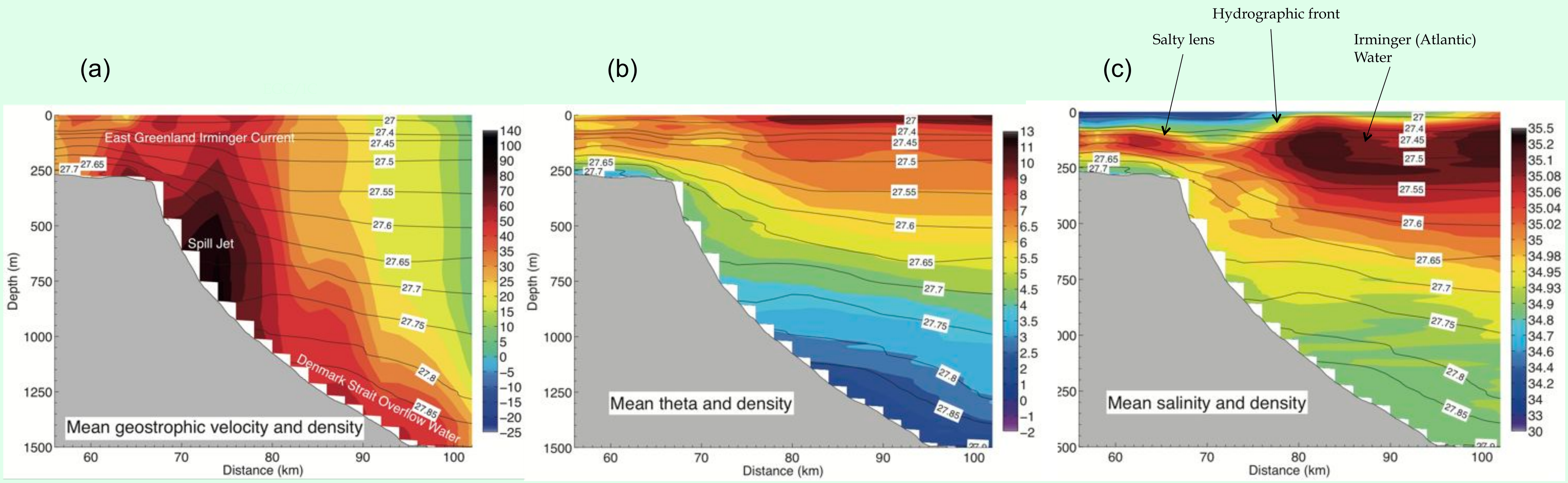

Figure 3: Mean vertical sections of (a) absolute geostrophic velocity (cm/s), referenced to vessel-mounted ADCP, (b) potential temperature (°C) and (c) salinity. Each plot is overlain by potential density (kg/m^3).

References and Acknowledgements

Brearley, J.A. et al. (2012) Deep Sea Res. 63, 1-19.

Defant, A. (1930) Phys.-Math. Klasse, XVI, 230–235.

Harden, B.E. and Pickart, R.S. (2011) Proc. 11th AMS Conf. on Polar Met. and Ocean.

The authors thank Dan Torres, Terry McKee and Paula Fratantoni (WHOI) for processing the ADCP data. The work was funded by NSF Grant OCE-0722694. Additional funding was provided by the Southampton-Woods Hole Exchange Program and the Royal Meterological Society.

3 Variability in Boundary Current Transport and T/S Properties

Substantial variability occurs in both the position of the boundary current components and their transport between the individual section occupations (Table 1). In 2001 and 2003 the hydrographic front was located far onshore allowing warm subtropical-origin water to penetrate onto the shelf and shifting the Spill Jet onto the outer shelf (Figure 4a-d). By contrast, in 2004 and 2007 the hydrographic front resided much further offshore (Figure 4e-h) and the extremely steep isopycnal slope at the shelf break leads to a very strong Spill Jet (peak velocities exceed 150 cm/s – see Figure 5). Nevertheless, the feature is very narrow (<20 km).

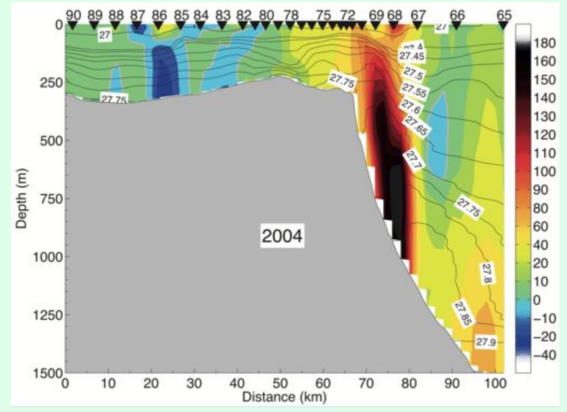

Figure 5: Geostrophic transport (cm/s), referenced to vessel mounted ADCP, for 2004.

	EGIC	SPILL JET	DWBC
2001	8.2	2.7	7.1
2003	10.7	2,2	5.8
2004	5.0	10.4	5.6
2007	3.1	4.6	1.6
Mean±ADCP error	6.8±0.9	5.0±0.3	4.9±0.5

Table 1: Volume transports of boundary current components by year (Sv).

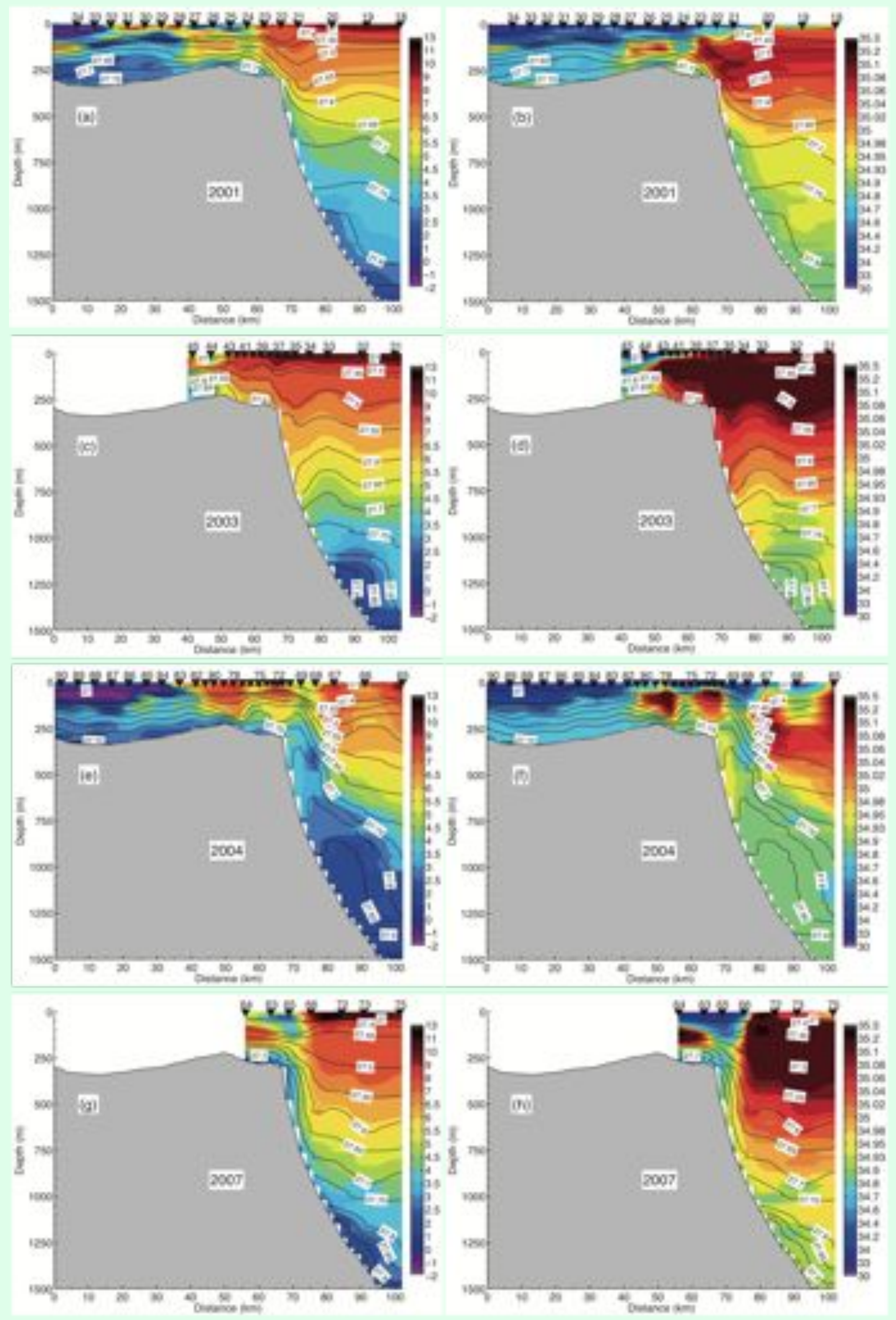

Figure 4: Vertical sections of salinity and potential temperature (in °C) along the spill jet section: (a), (c), (e) and (g) display potential temperature in 2001, 2003, 2004 and 2007 respectively, whilst (b), (d) and (f) and (h) show salinity in those years. σ_θ surfaces in kg m^{-3} are overlaid and station numbers are given for each panel.

The spill Jet is colder, fresher and denser in 2004 and 2007 than in 2001 and 2003 (Figure 6). This occurs when the hydrographic front is located further offshore; at these times the density of part of the spill jet exceeds σ_θ = 27.8 (the range of DSOW). In 2004 and 2007, the spill jet is the largest individual component of the boundary current (Table 1).

Given the close proximity of warm /salty and cold/fresh water, the jet is subject to double diffusive processes, which may eventually contribute to the reversal of the offshore density gradient by the time the boundary current reaches Cape Farewell (Figure 7).

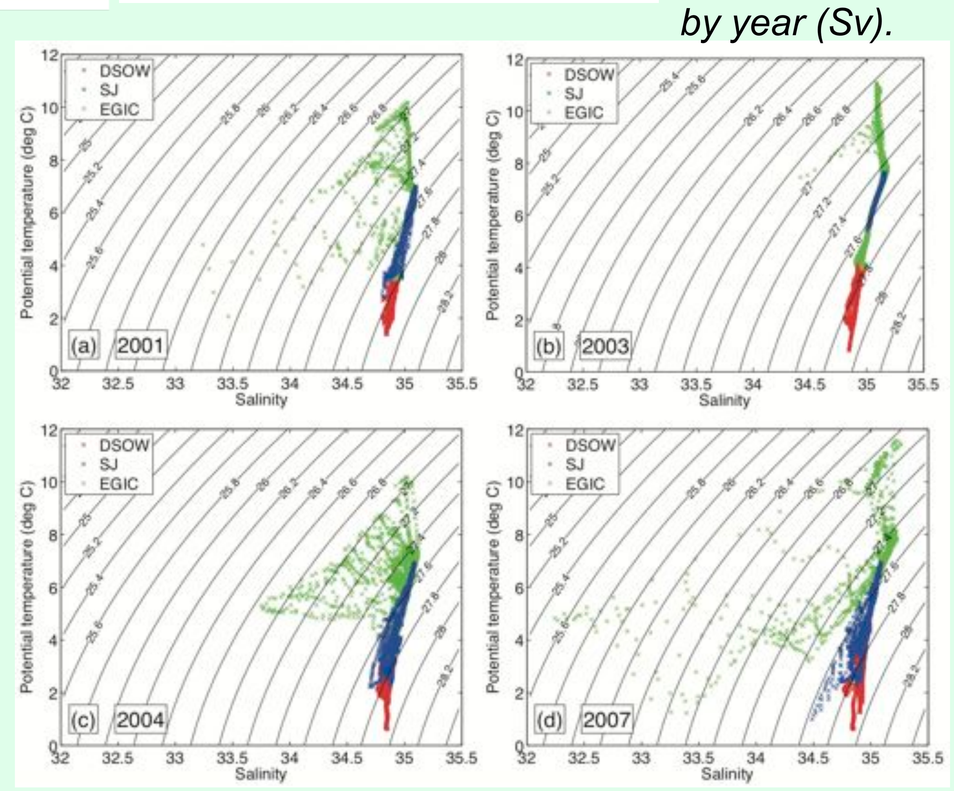

Figure 6: θ/S diagram of the boundary current for the years (a) 2001; (b) 2003; (c) 2004 and (d) 2007, with three separate components of the boundary current colour-coded accordingly. Density contours are plotted.

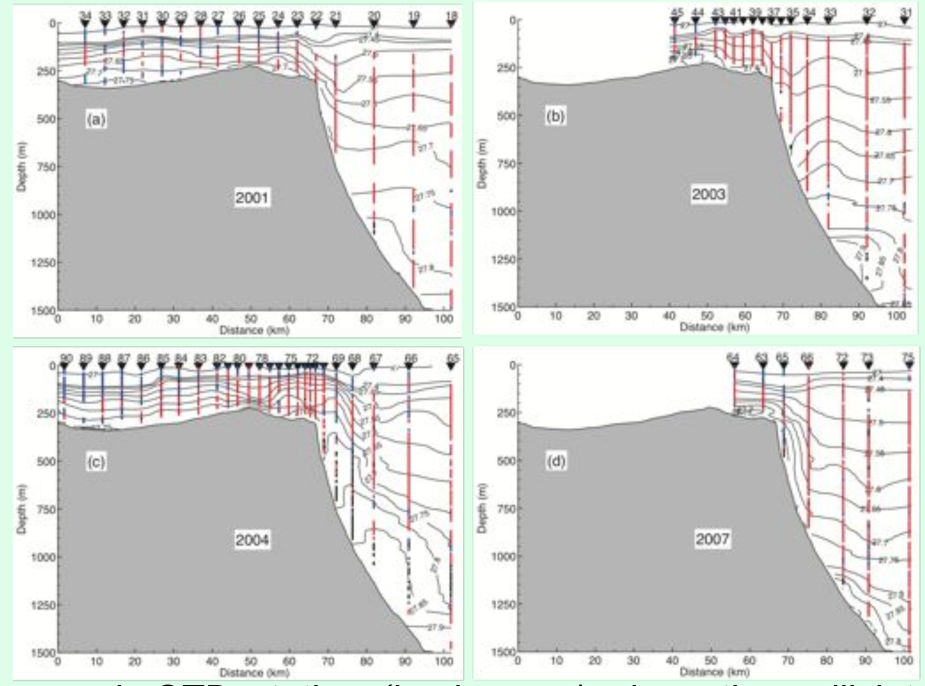

Figure 7: Turner angles from each CTD station (in degrees) along the spill jet section. Red areas denote regions subject to salt fingering (45° < Tu < 90°), blue areas denote regions susceptible to diffusive convection (–90° < Tu < –45°) and black areas denote regions of possible static instability (Tu < –90° or Tu > 90°).

4 Mixing and Instability in the Boundary Current

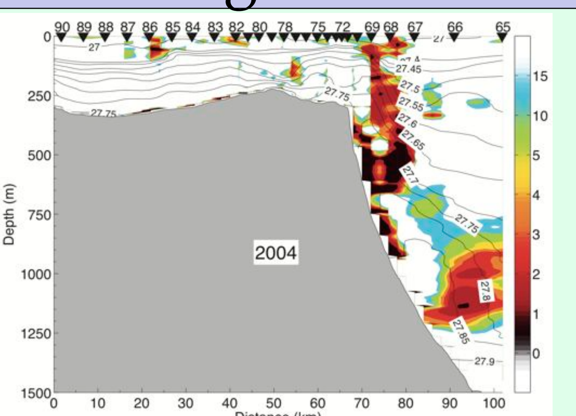

Figure 8: Gradient Richardson Number for the 2004 occupation. Dark red areas denote regions where Ri <1.

The spill jet is subject to a number of instability processes that cause intense lateral mixing (Figure 8):

1. Symmetric instability which acts on timescales of 2h, seen by ς/f being less than -1 on the inshore flank of the spill jet.
2. Slower-developing baroclinic instability, seen by the sign of the total PV gradient changing across the spill jet in every year.

Lateral exchange associated with the cascading of dense water off the shelf is important in setting the final transport and properties of the currents along the slope of the Irminger Sea. It is thus possible that a change in the composition of shelf water flowing through Denmark Strait in response to enhanced FW discharge could influence the intermediate, and possibly deep limbs of the overturning circulation.

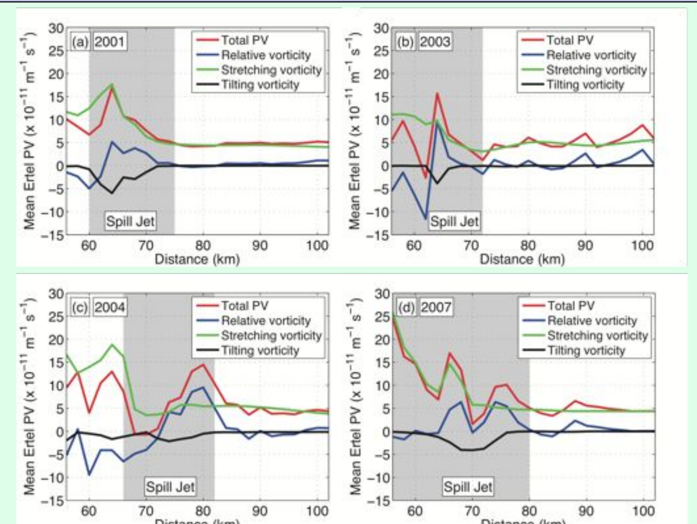

Figure 9: Total potential vorticity (PV) budget in the depth range of the spill jet.